Available online at www.sciencedirect.com
SCIENCE DIRECT®
Catalysis Today 98 (2004) 441–446
CATALYSIS TODAY
www.elsevier.com/locate/cattod

Discoloration and mineralization of Orange II by using Fe^{3+}-doped TiO_2 and bentonite clay-based Fe nanocatalysts

Jiyun Feng, Raymond S.K. Wong, Xijun Hu, Po Lock Yue*

Department of Chemical Engineering, Hong Kong University of Science and Technology, Clear Water Bay, Kowloon, Hong Kong

Available online 27 September 2004

Abstract

Nanostructured catalysts (Fe^{3+}-doped TiO_2 and bentonite clay-based Fe nanocomposite (Fe–B)) have been developed for the discoloration and mineralization of a non-biodegradable azo dye, Orange II. The Fe^{3+}-doped TiO_2 nanocatalysts synthesized by the sol–gel method and the Fe–B nanocatalyst by the pillaring method were characterized by X-ray diffraction (XRD), X-ray photoelectron spectroscopy (XPS), X-ray reflective fluorescence (XRF), and the BET method. Their photocatalytic activities for the discoloration and mineralization of a non-biodegradable azo dye Orange II were evaluated. The results indicate that the concentration of Fe^{3+} dopant does not influence the crystal structure of the nanocatalysts, but significantly affect their photocatalytic activity. The best efficiency for both discoloration and mineralization of 0.2 mM Orange II was obtained by the 0.05 at.% Fe^{3+}-doped TiO_2 nanocatalyst. The nanostructured Fe–B catalyst exhibits good catalytic activity in the discoloration and mineralization of Orange II in the presence of UVC light (254 nm) and H_2O_2 at an initial solution pH of 6.60, with negligible leaching of Fe ions from the nanocatalyst. This result has demonstrated that it is feasible to use the Fe–B nanocatalyst as a heterogeneous photo-Fenton catalyst for practical industrial wastewater treatment, without the need for pre-adjustment of solution pH and removal of Fe^{3+} ions after the reaction.

Keywords: Nanostructured; TiO_2; Photo-Fenton; Orange II

1. Introduction

Nanostructured materials have received much attention in the last decade due to their unique physical, chemical and electronic properties. Nanostructured materials have been developed and employed as heterogeneous catalysts for various applications including the remediation of water and air [1–14] by photocatalysis and photo-Fenton reaction. Photocatalysis is based on photogenerated electrons (e^-) and holes (h^+) migrating to the catalyst surface, reacting with adsorbed pollutants and resulting in the degradation of the pollutants. Undoubtedly, the most extensively studied nanostructured photocatalyst is TiO_2, which has been found to be capable of decomposing many organic compounds in the gas phase and the liquid phase. Obviously, reducing electron–hole recombination is a key for enhancing the photocatalytic activity of the catalyst. To achieve this goal, introducing defects into the TiO_2 lattice by metal ion dopants has been attempted. Many transition metal ions have been used for doping TiO_2 [1–7]. In particular, the potential enhancement effect of Fe^{3+} ions has been studied extensively. However, there are conflicting results obtained with Fe^{3+}-doped TiO_2. For example, Palmisano et al. [2] found that Fe^{3+} doping has no significant influence on the photocatalytic oxidation of 4-nitrophenol, while Choi et al. [4] observed that a small amount of Fe^{3+} doping enhanced the photocatalytic activity of TiO_2 in the oxidation of $CHCl_3$. Zhang et al. [7] found that the optimal Fe^{3+} dopant concentration for enhancing catalytic activity strongly depended on the particle size of the TiO_2 nanocatalyst. The optimal Fe^{3+} concentration was found to decrease with increasing particle size.

Apart from TiO_2 nanostructured catalysts, clay-based nanostructured catalysts have also been developed for both water and air remediation [9–14]. For example, Feng et al. [11–14] synthesized laponite and bentonite clay-based Fe

* Corresponding author. Tel.: +852 2358 7130; fax: +852 2358 0054.
E-mail address: keplyue@ust.hk (P.L. Yue).

0920-5861/$ – see front matter © 2004 Elsevier B.V. All rights reserved.
doi:10.1016/j.cattod.2004.08.007

nanocomposites using the so-called pillaring technique and used them as heterogeneous nanocatalysts for the photo-Fenton discoloration and mineralization of azo dyes such as Orange II and Reactive Red HE-3B in the presence of UVC light and H_2O_2. Their results illustrate that both nanocatalysts exhibited optimal photocatalytic activity at an initial solution of pH 3.0, which is the optimal pH for homogeneous and heterogeneous photo-Fenton reactions [15–18]. For the application of photo-Fenton reaction to the treatment of industrial wastewater, the pH of the wastewater would need to be adjusted to obtain the optimal efficiency. At low pH, the leaching of Fe ions from a heterogeneous photo-Fenton catalyst cannot be completely eliminated. It would be of considerable interest to investigate how the catalysts might perform at higher pH, i.e. nearer to neutral pH, such that pre-adjustment of the wastewater would not be required.

In the present work, Fe^{3+}-doped TiO_2 nanocatalysts, and bentonite clay-based Fe nanocatalyst (Fe–B) were prepared by the sol–gel and pillaring methods, respectively. Both catalysts were characterized by XRD, XPS, XRD and BET methods. The photocatalytic activities of the Fe^{3+}-doped TiO_2 nanocatalysts for the discoloration and mineralization of 0.2 mM Orange II in the presence of UVC light and O_2 were evaluated. The effect of Fe^{3+} dopant concentration on the photocatalytic activities of the doped TiO_2 nanocatalysts was studied. The photocatalytic activity of the Fe–B nanocatalyst at an initially nearly neutral pH was also examined.

2. Experimental

2.1. Chemicals

Titanium (IV) isopropoxide (TIP, $Ti(OCH(CH_3)_2)_4$), isopropanol, H_2O_2 (30%), $Fe(NO_3)_3{\cdot}9H_2O$, and Na_2CO_3 were all obtained from Aldrich. The layered clay used in this study was bentonite.

2.2. Synthesis of Fe^{3+}-doped TiO_2 and Fe–B nanocatalysts

The Fe^{3+}-doped TiO_2 nanocatalyst was synthesized by using a typical sol–gel method. A calculated amount of Fe^{3+} (using $Fe(NO_3)_3{\cdot}9H_2O$) was first added to an alcohol–water mixture prior to the hydrolysis of TIP. The hydrolysis of TIP was then performed by adding TIP drop by drop to a mixed isopropanol–water solution under vigorous stirring in a nitrogen environment for 1 h. The molar ratio of water to TIP was 95. The precipitated gels were collected by centrifugation and rinsed with ultra-pure water. The precipitates were dried at 80 °C overnight, and finally calcined at 450 °C for 3 h in air. The Fe–B nanocatalyst was synthesized by using the previously described pillaring technique [11–14].

2.3. Characterization of Fe^{3+}-doped TiO_2 and Fe–B nanocatalysts

XRD powder diffraction measurements of both the Fe^{3+}-doped TiO_2 and Fe–B nanocatalysts were performed using a powder diffractometer (Model: Philips PW 1830) equipped with a Cu Kα radiation. The accelerating voltage and current used were 40 kV and 20 mA, respectively. The 2θ ranged from 10 to 70°.

The Fe concentration on the surface of the Fe^{3+}-doped TiO_2 and Fe–B nanocatalysts was analyzed by a PHI 5600 spectrometer. The take-off angle used was 45°.

The bulk Fe concentration of the Fe–B nanocatalyst was determined by a JOEL X-ray Reflective Fluorescence spectrometer (XRF) (Model: JSX 3201Z).

The specific surface areas of both the Fe^{3+}-doped TiO_2 nanocatalysts and the Fe–B nanocatalyst were measured at 77 K using the BET method performed on an Omnisorp 100CX BET machine.

2.4. Evaluation of the Fe^{3+}-doped TiO_2 and Fe–B nanocatalysts

The evaluation of the Fe^{3+}-doped TiO_2 nanocatalysts was conducted in a batch photoreactor. The reactor is cylindrical with two 8 W UVC lamps inserted in the center of the reactor [11]. The model pollutant was an azo dye Orange II that is widely used in textile industry. It is non-biodegradable and does not photodegrade under UV illumination. The total volume of the reaction solution was 0.4 L, the initial Orange II concentration used was 0.2 mM, the O_2 flow rate was 10 L/min, and the Fe^{3+}-doped TiO_2 nanocatalyst loading was 0.5 g/L.

For the evaluation of the Fe–B nanocatalyst, a similar batch photoreactor was used [14]. The total volume of reaction solution was 0.5 L, the initial Orange II concentration was also 0.2 mM, the H_2O_2 concentration was 10 mM, the Fe–B nanocatalyst loading was 1.0 g/L, and the initial solution pH was adjusted to 6.60 by using diluted NaOH solution. The concentration of H_2O_2 used was optimal [14]. Only one 8 W UVC lamp was used as the light source.

The UV–vis spectrum of Orange II shows the maximum absorption peak at 486 nm [11,14], thus the Orange II concentration in the solution can be determined by measuring the absorbance at 486 nm using a UV–vis spectrophotometer (Shimadzu UV Mini 1240). Prior to the measurements, a calibration curve was obtained by using standard Orange II solutions with known concentrations. A linear relationship between absorbance at 486 nm and Orange II concentration was obtained up to 0.1 mM Orange II. Because the reaction continued after sampling, the measurement of absorbance of reaction solution should be completed within 1 min.

For the same reason, after sampling, the sample for total organic carbon (TOC) measurements was immediately treated with a scavenging reagent (0.02 M Na_2SO_3, 0.02 M

KH_2PO_4, 0.02 M KI and 0.01 M NaOH) of the same volume. The TOC of the reaction solution was measured with a Shimadzu TOC-5000 A analyzer equipped with an auto-sampler. The experimental errors in the TOC measurement were less than 10%.

3. Results and discussion

3.1. Characterization of the Fe^{3+}-doped TiO_2 and Fe–B nanocatalysts

The Fe^{3+}-doped TiO_2 nanocatalysts were first characterized by XRD. Our results show that only anatase-phase TiO_2 was detected, indicating that the introduction of Fe^{3+} as dopant does not alter the crystal structure of the TiO_2 nanocatalysts. The primary particle size of the Fe^{3+}-doped TiO_2 nanocatalysts as determined by the peak broadening method ranged from 11 to 13 nm. The surface Fe^{3+} concentrations of the nanocatalysts were measured by XPS and the results are shown in Table 1. The specific surface area of the Fe^{3+}-doped nanocatalysts as determined by the BET method ranged from 110 to 130 m^2/g, indicating that the Fe^{3+} ions also do not markedly influence the BET surface area of the TiO_2 nanocatalysts.

The Fe–B nanocatalyst was also characterized by XRD. Fig. 1 shows the XRD pattern of the Fe–B nanocatalyst. Based on the main diffraction peaks, it is deduced that the Fe–B nanocatalyst mainly consists of Fe_2O_3 (hematite) and SiO_2 (quartz) crystallites, respectively. The bulk Fe concentration with respect to the total mass of Fe–B nanocatalyst as determined by XRF was 31.8% (wt.%). The Fe surface atomic concentration of the Fe–B nanocatalyst determined by XPS was 12.3%. The specific surface area measured by the BET method was 250 m^2/g. The particle size of the Fe–B nanocatalyst as determined by TEM ranged from 20 to 200 nm [14].

3.2. Evaluation of the Fe^{3+}-doped TiO_2 nanocatalysts

The photocatalytic activities of the Fe^{3+}-doped TiO_2 nanocatalysts for the discoloration and mineralization of 0.2 mM Orange II were evaluated in the presence of 0.5 g Fe^{3+}-doped TiO_2 nanocatalyst/L, 2 × 8 W UVC, and an O_2 flow rate of 10 L/min. The results are shown in Figs. 2 and 3, respectively. It can be seen from Fig. 2 that the discoloration kinetics of 0.2 mM Orange II are significantly influenced by the Fe^{3+} dopant concentration. When compared with the undoped TiO_2 nanocatalyst (curve b), a 0.05 at.% Fe^{3+}-doped TiO_2 nanocatalyst exhibits a significantly enhanced photocatalytic activity – 100% color removal is achieved after 150 min of reaction. This result agrees well with previously published results [4,7]. The enhanced photocatalytic activity could be attributed to the fact that the recombination of e^- and h^+ was reduced. However, as the Fe^{3+} dopant concentration increased from 0.10 to 0.50 at.%, the discoloration kinetics (curves d and e) were found not to have been significantly enhanced (curve b), which is in line with the results reported by Palmisano et al. [2]. When the dopant Fe^{3+} concentration further increased to 1.0 at.%, a much slower discoloration kinetics (curve f) was observed, indicating that a high Fe^{3+} dopant concentration (1.0 at.%) is detrimental to the photocatalytic activity of TiO_2 nanocatalyst. This is because at too high Fe^{3+} dopant concentration,

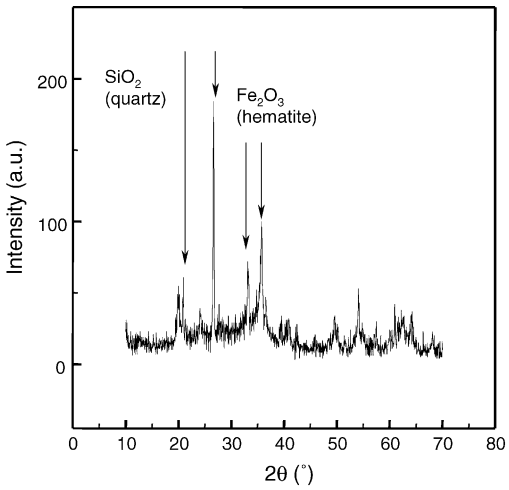

Fig. 1. XRD pattern of Fe–B nanocatalyst.

Table 1
Surface Fe atomic concentration (at.%) of the Fe^{3+}-doped TiO_2 nanocatalysts by XPS

Dopant Fe^{3+} (at.%)	0.00	0.05	0.10	0.50	1.0
Surface Fe^{3+} (at.%)	0.00	0.04	0.13	0.16	0.37

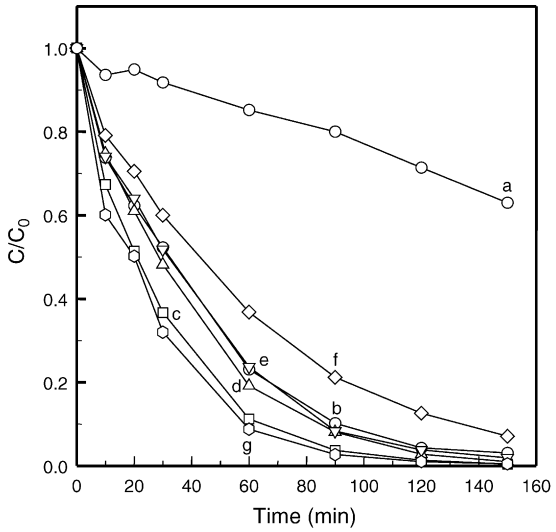

Fig. 2. Discoloration of 0.2 mM Orange II in the presence of 2 × 8 W UVC, 0.5 g/L Fe^{3+}-doped TiO_2 nanocatalysts, and an O_2 flow rate of 10 L/min: (a) only with UVC; (b) undoped TiO_2; (c) 0.05 at.% Fe^{3+}-doped TiO_2; (d) 0.10 at.% Fe^{3+}-doped TiO_2; (e) 0.50 at.% Fe^{3+}-doped TiO_2; (f) 1.0 at.% Fe^{3+}-doped TiO_2; (g) Degussa P25.

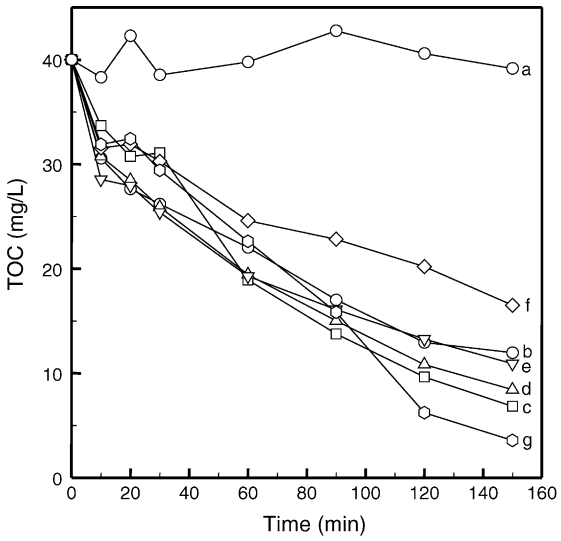

Fig. 3. Mineralization of 0.2 mM Orange II in the presence of 2 × 8 W UVC, 0.5 g/L Fe^{3+}-doped TiO_2 nanocatalysts, and an O_2 flow rate of 10 L/min: (a) only with UVC; (b) undoped TiO_2; (c) 0.05 at.% Fe^{3+}-doped TiO_2; (d) 0.10 at.% Fe^{3+}-doped TiO_2; (e) 0.50 at.% Fe^{3+}-doped TiO_2; (f) 1.0 at.% Fe^{3+}-doped TiO_2; (g) Degussa P25.

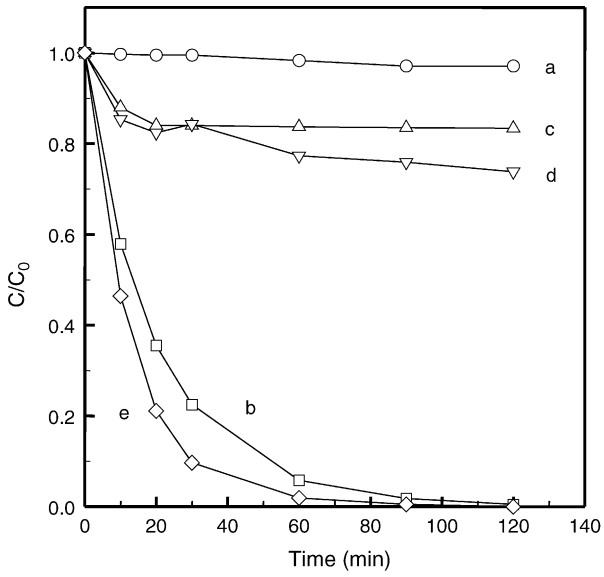

Fig. 4. Discoloration of 0.2 mM Orange II by using Fe–B nanocatalyst at an initial solution pH 6.60: (a) only with 8 W UVC; (b) 10 mM H_2O_2 and 8 W UVC; (c) only with 1.0 g Fe–B nanocatalyst/L in the dark; (d) 10 mM H_2O_2 and 1.0 g Fe–B nanocatalyst/L in the dark; (e) 10 mM H_2O_2, 1.0 g Fe–B nanocatalyst/L, and 8 W UVC.

a hole can be trapped more than once on its way to the catalyst surface so that its apparent mobility may become very slow, making the recombination with an electron more likely [7]. In addition, when compared with Degussa P25, the best Fe^{3+}-doped TiO_2 exhibited similar photocatalytic activity for the discoloration of 0.2 mM Orange II.

For the mineralization of 0.2 mM Orange II, as shown in Fig. 3, similar trends were observed. Compared with the undoped TiO_2 nanocatalyst (curve b), it can also be seen that the 0.05 at.% Fe^{3+}-doped TiO_2 nanocatalyst exhibits the best catalytic efficiency (curve c) – more than 75% TOC removal was achieved after 150 min. As the Fe^{3+} dopant concentration increases, the photocatalytic mineralization activity of the doped TiO_2 nanocatalyst decreases rapidly (see curves d–f). When compared with the 'standard' Degussa P25, the best Fe^{3+}-doped TiO_2 exhibited similar photocatalytic activity for the mineralization of 0.2 mM Orange II.

In summary, only the 0.05 at.% Fe^{3+}-doped TiO_2 nanocatalyst exhibits enhanced photocatalytic activity for both discoloration and mineralization of 0.2 mM Orange II.

3.3. Evaluation of the Fe–B nanocatalyst

The photocatalytic activity of the Fe–B nanocatalyst was evaluated for the discoloration and mineralization of 0.2 mM Orange II in the presence of 10 mM H_2O_2, 1.0 g Fe–B/L, and 8 W UVC at an initial solution pH of 6.60. The purpose of using this initial solution pH of 6.60 is to examine the activity of the Fe–B nanocatalyst at nearly neutral pH. It is well accepted that the photo-Fenton reaction exhibits the best efficiency in the oxidation of organic pollutants at a solution pH between 2.8 and 3.2 [15–18], thus necessitating a pre-adjustment of the initial solution pH of industrial wastewater from neutral to about 3, and raising the treatment cost.

Fig. 4 shows the discoloration kinetics of 0.2 mM Orange II under different conditions. Several observations were made. First, with one 8 W UVC lamp, but without the Fe–B catalyst and H_2O_2 (curve a), the discoloration of 0.2 mM Orange II is insignificant, indicating that Orange II itself can resist UV light. Second, with 10 mM H_2O_2 and one 8 W UVC lamp but without the Fe–B catalyst (curve b), the discoloration of 0.2 mM Orange II is significant. After 120 min, complete discoloration of 0.2 mM Orange II was achieved. This observed discoloration results from the oxidation of Orange II by the OH radicals generated by photolytic peroxidation (UVC and H_2O_2) as shown in the following equations:

$$H_2O_2 + \text{UVClight} \rightarrow 2^{\bullet}\text{OH} \quad (1)$$

$$^{\bullet}\text{OH} + \text{OrangeII} \rightarrow \text{reactionintermediates} \rightarrow H_2O + CO_2 + \text{inorganicions} \quad (2)$$

Third, without UV light and H_2O_2 but with 1.0 g Fe–B/L in the dark (curve c), the concentration of Orange II decreased quite fast in the first 20 min and then attained an asymptotic value. The discoloration of 0.2 mM Orange II observed here can be attributed to the adsorption of Orange II on the surface of Fe–B nanocatalyst. The adsorption capacity of the Fe–B nanocatalyst at initial solution pH of 6.60 was found to be 10.5 mg Orange II/g Fe–B nanocatalyst. Fourth, without UV light but with 10 mM H_2O_2 and 1.0 g Fe–B/L in the dark (curve d), the concentration of Orange II decreased

in the first 20 min, followed by a slow continuous decrease. The decrease in Orange II in the first 20 min is again caused by the adsorption of Orange II on the surface of Fe–B nanocatalyst. The subsequent decrease after 20 min resulted from oxidation of Orange II by OH radicals coming from the ''dark'' Fenton reaction. It can be seen that the dark Fenton reaction does not give rise to fast discoloration of Orange II. Finally, with 1.0 g Fe–B/L nanocatalyst, 10 mM H_2O_2, and one 8 W UVC lamp (curve e), the discoloration of 0.2 mM Orange II is very fast. After 90 min of reaction, 100% discoloration of 0.2 mM Orange II was achieved. The leaching of Fe ions from the Fe–B at this initial solution pH of 6.60 is negligible. With a sufficiently high activity and negligible loss of Fe ions from the Fe–B nanocatalysts, a practical treatment process becomes feasible.

Complete discoloration of 0.2 mM Orange II does not mean that all Orange II molecules have been oxidized to CO_2, H_2O and inorganic ions. This is because colorless reaction intermediates can be formed and the intermediates might not be environmentally acceptable. Therefore, the removal of total organic carbon, TOC, is as important as color removal. Fig. 5 depicts the mineralization kinetics of 0.2 mM Orange II under different conditions. Without H_2O_2 and Fe–B nanocatalyst but only with one 8 W UVC lamp (curve a), the TOC of 0.2 mM Orange II did not decrease at all after 120 min reaction, further confirming that Orange II can resist UV light. Without the Fe–B nanocatalyst but with 10 mM H_2O_2 and one 8 W UVC lamp (curve b), the TOC of 0.2 mM Orange II decreased from 40 to around 31 mg/L after 120 min. More than 75% TOC still remains in solution, indicating that with 10 mM H_2O_2 + 8 W UVC light (photolytic peroxidation), Orange II cannot be effectively mineralized. The limited mineralization of 0.2 mM Orange II under this condition is due to the fact that the OH radicals formed in solution are short-lived, and many of them decay before they meet the intermediates in the solution. Without H_2O_2 and UVC but with 1.0 g Fe–B nanocatalyst/L (curve c), and without UVC but with 10 mM H_2O_2 and 1.0 g Fe–B nanocatalyst/L (curve d), the TOC reductions observed after 120 min were mainly due to the adsorption of the organics on the surface of the Fe–B nanocatalyst. However, with 10 mM H_2O_2, 1.0 g Fe–B nanocatalyst/L, and one 8 W UVC lamp, the TOC decreased from 40 to 16 mg/L after 120 min, indicating more than 65% TOC were removed. This result also shows that the Fe–B nanocatalyst exhibits a good photocatalytic activity for the mineralization of Orange II. The Fe–B nanocatalyst for the heterogeneous photo-Fenton is effective for the mineralization of Orange II because the intermediates are adsorbed on the catalyst and are more readily mineralized by the OH radicals formed on the surface of the Fe–B nanocatalyst.

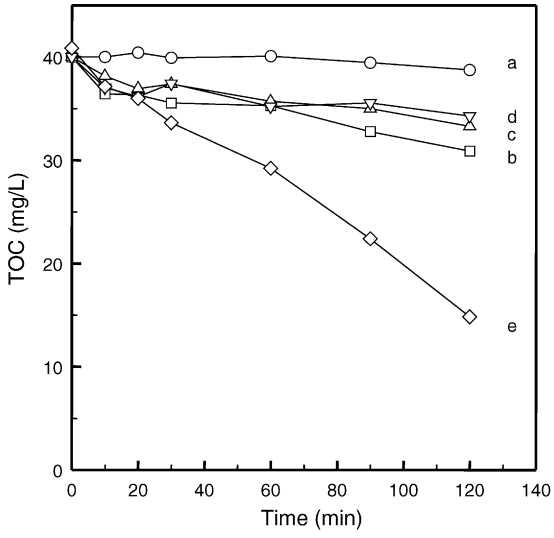

Fig. 5. Mineralization of 0.2 mM Orange II by using Fe–B nanocatalysts nanocatalyst at an initial solution pH 6.60: (a) only with 8 W UVC; (b) 10 mM H_2O_2 and 8 W UVC; (c) only with 1.0 g Fe–B nanocatalyst/L in the dark; (d) 10 mM H_2O_2 and 1.0 g Fe–B nanocatalyst/L in the dark; (e) 10 mM H_2O_2, 1.0 g Fe–B nanocatalyst/L, and 8 W UVC.

An attempt is made to elucidate the reason for the good photocatalytic activity of the Fe–B nanocatalyst at an initial solution pH of 6.60. The solution pH before and after reaction was measured. It was found that the solution pH changed from 6.60 to 4.40, indicating that during the discoloration and mineralization of 0.2 mM Orange II, some acidic intermediates and products are formed. The formation of acidic products can be expressed by the following equation [11]:

$$C_{16}H_{11}N_2NaO_4S + 42H_2O_2 \rightarrow 16CO_2 + 46H_2O + 2HNO_3 + NaHSO_4 \quad (3)$$

Both HNO_3 and HSO_4^- would cause a significant decrease in the solution pH, which allows the Fe–B nanocatalyst to exhibit a reasonably good photocatalytic activity but with only a negligible loss of Fe ions leached from the catalyst into solution, even though the initial solution is almost at neutral pH.

4. Conclusions

Nanostructured Fe^{3+}-doped TiO_2, and bentonite clay-based Fe nanocatalysts have been synthesized by sol–gel and pillaring methods for environmental applications, and were characterized by X-ray diffraction (XRD), X-ray photoelectron spectroscopy (XPS), X-ray reflective fluorescence (XRF) and the BET method. Their photocatalytic activities were evaluated for the discoloration and mineralization of a non-biodegradable azo dye Orange II. Our results indicate that the Fe^{3+} dopant does not change the crystal structure of the TiO_2 nanocatalysts, but significantly affect their photocatalytic activity. A TiO_2 nanocatalyst doped with 0.05 at.% Fe^{3+} gives the optimal efficiency for both discoloration and mineralization of 0.2 mM Orange II. The activity of the nanostructured Fe–B catalyst is reasonably high at an initial solution pH of 6.6. At this pH, there is

negligible leaching of Fe ions from the nanocatalyst. This result illustrates that it is feasible to use the Fe–B nanocatalyst for the treatment of industrial wastewater by a heterogeneous photo-Fenton process, without the pre-adjustment of solution pH and removal of Fe^{3+} from the wastewater after reaction.

Acknowledgements

This work was supported by the Hong Kong Innovation and Technology Fund (ITF) under the grant ITS176/01C, and the Hong Kong Government Research Grant Council (RGC) under the grant HKUST6074/01P.

References

[1] M. Gratzel, F.H. Russel, J. Phys. Chem. (1990) 94.
[2] L. Palmisano, M. Schiavello, A. Sclafani, C. Martin, I. Martin, V. Rives, Catal. Lett. 24 (1994) 303–315.
[3] A. Milis, J. Peral, J. Domenech, J. Mol. Catal. 87 (1994) 67–74.
[4] W. Choi, A. Termin, M.R. Hoffmann, J. Phys. Chem. 98 (1994) 13669–13679.
[5] M.I. Litter, J.A. Navio, J. Photochem. Photobiol. A 98 (1996) 171–181.
[6] C.C. Wang, Z. Zhang, J.Y. Ying, Nanostruct. Mater. 9 (1997) 583–586.
[7] Z. Zhang, C. Wang, R. Zakria, J.Y. Ying, J. Phys. Chem. B 102 (1998) 10871–10878.
[8] A.J. Maira, K.L. Yeung, C.Y. Lee, P.L. Yue, C.K. Chan, J. Catal. 192 (2000) 185–196.
[9] S. Wang, H.Y. Zhu, G.Q. Lu, J. Colloid. Interf. Sci. 204 (1998) 128–134.
[10] H.Y. Zhu, G.Q. Lu, Langmuir 17 (2001) 588–594.
[11] J.Y. Feng, X. Hu, P.L. Yue, H.Y. Zhu, G.Q. Lu, Ind. Eng. Chem. Res. 42 (2003) 2058–2066.
[12] J.Y. Feng, X. Hu, P.L. Yue, H.Y. Zhu, G.Q. Lu, Chem. Eng. Sci. 58 (2003) 679–685.
[13] J.Y. Feng, X. Hu, P.L. Yue, H.Y. Zhu, G.Q. Lu, Water Res. 37 (2003) 3776–3784.
[14] J.Y. Feng, X. Hu, P.L. Yue, Environ. Sci. Technol. 38 (2004) 269–275.
[15] J.J. Pignatello, Environ. Sci. Technol. 26 (1992) 944–951.
[16] B. Ruppert, R. Bauer, G. Heisler, S. Novalic, Chemosphere 3 (1993) 339–347.
[17] N.H. Ince, G. Tezcanli, Water Sci. Technol. 40 (1999) 183–190.
[18] J.L. Acero, F.J. Benitez, F.J. Real, A.L. Leal, Water Sci. Technol. 44 (2001) 31–38.